Structural Engineering and Mechanics, Vol. 6, No. 5 (1998) 529-542
DOI: http://dx.doi.org/10.12989/sem.1998.6.5.529

Piezothermoelastic solution for angle-ply laminated plate in cylindrical bending

G.P. Dube†, M.M. Upadhyay‡, P.C. Dumir‡†, and S. Kumar‡

Applied Mechanics Department, I.I.T. Delhi, New Delhi-110016, India

Abstract. Generalised plane strain solution is presented for simply supported, angle-ply laminated hybrid plate under cylindrical bending. The arbitrary constants in the general solution of the governing differential equations are obtained from the boundary and interface conditions. The response of hybrid plates to sinusoidal loads is obtained to illustrate the effect of the thickness parameter and the ply-angle. The classical lamination theory and the first order shear deformation theory are also assessed.

Key words: piezothermoelectric response; cylindrical bending; angle-ply plate; laminated plate; simply supported plate.

1. Introduction

There is current interest to quantify the performance of smart plates with piezoeletric layers. Three dimensional (3D) solutions are needed to assess two dimensional (2D) plate theories for thermoelectroelastic analysis. Ray *et al.* (1992, 1993a) and Brooks and Heyliger (1994) presented exact plane strain solution for simply supported single layer and cross-ply laminated piezoelectric plates with distributed and patched actuators. Ashida *et al.* (1994a, 1994b) have presented general plane strain solution of piezothermoelastic problems in orthotropic plates of crystal class mm2 in terms of potential functions and solved direct and inverse problems of infinite plate subjected to heating on one surface and electric surface charge on both surfaces. Piezothermoelastic plane strain solutions for single layer and hybrid cross-ply infinite flat panel have been developed by Dube *et al.* (1996) and Kapuria *et al.* (1997). Tang *et al.* (1996) have assessed 2D plate theories for rectangular hybrid cross-ply plates in the light of 3D solutions [Ray *et al.* (1993b), Heyliger (1994), Xu *et al.* (1995)]. Pagano (1970) developed 3D solution for simply supported angle-ply laminated composite plate in cylindrical bending under mechanical load. There is no solution available for angle-ply laminated hybrid composite piezoelectric plates.

We present generalised plane strain solution for cylindrical bending of simply supported, hybrid angle-ply laminated plate using mixed formulation. The arbitrary constants in the general solution for each layer and the unknown extraneous charge densities at the interfaces where potential or potential difference is prescribed are determined from the boundary and interface conditions. Numerical results are presented for sinusoidal loads to illustrate the effect

† Associate Professor
‡ Graduate Student
‡† Professor

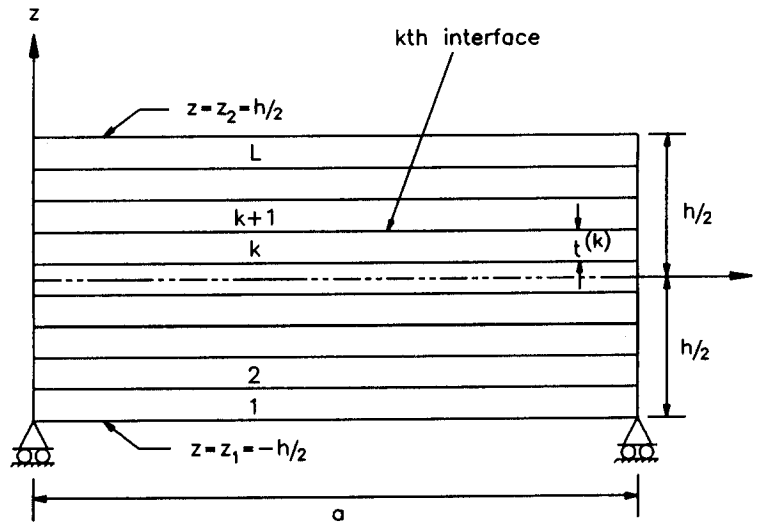

Fig. 1 Geometry of hybrid plate

of the thickness parameter and the ply orientation. The generalised plane strain solution has been used to assess 2D classical lamination theory (CLT) and first order shear deformation theory (FSDT) for angle-ply laminated hybrid plate.

2. Governing equations

Consider an infinitely long simply supported L-layered angle-ply laminated plate of span a and thickness h as shown in Fig. 1. The bottom face of the first layer is at $z=z_1=-h/2$ and the top face of the Lth layer is at $z=z_2=h/2$. The interface between the kth and the $(k+1)$th layer is named as the kth interface. Let the thickness of kth layer be $t^{(k)}$. The layer superscript is omitted unless needed for clarity. The transverse displacement w and the tractions in the inplane directions x and y are zero at the simply supported ends at $x=0$, a. These ends are electrically grounded and maintained at the stress-free reference temperature. The panel is subjected to electrothermomechanical load which does not vary along the longitudinal coordinate y. Thus all the entities in this generalised plane strain problem are independent of y. The layers can be elastic or piezoelectric exhibiting symmetry of orthorhombic crystal class mm2.

For linear piezoelectric medium, stress σ', strain ε', electric field E' and electric displacement D', with respect to principal material axes x_i, are related by

$$\varepsilon' = S\sigma' + d^T E' + \alpha T, \quad D' = d\sigma' + \varepsilon E' + qT \text{ where } \varepsilon = \eta + ed^T, \quad q = p + e\alpha, \quad e = dS^{-1}, \tag{1}$$

$$\sigma' = [\sigma_1\ \sigma_2\ \sigma_3\ \tau_{23}\ \tau_{31}\ \tau_{12}]^T, \quad E' = [E_1 E_2 E_3]^T, \quad \varepsilon' = [\varepsilon_1\ \varepsilon_2\ \varepsilon_3\ \gamma_{23}\ \gamma_{31}\ \gamma_{12}]^T, \quad D' = [D_1 D_2 D_3]^T. \tag{2}$$

The superscript T denotes matrix transpose and T is the temperature rise above the stress-free reference temperature. S, d, η, α, p are the matrices of elastic compliance, piezoelectric strain constants, permittivities, thermal expansion coefficients and pyroelectric constants. The dependence of material property on temperature is not included in this study. For orthotropic materials of class mm2, with poling in direction $x_3(z)$, the matrices of material constants with

respect to the principal axes x_i are given by:

$$\varepsilon=\begin{bmatrix}\varepsilon_{11} & 0 & 0\\ 0 & \varepsilon_{22} & 0\\ 0 & 0 & \varepsilon_{33}\end{bmatrix},\quad \eta=\begin{bmatrix}\eta_{11} & 0 & 0\\ 0 & \eta_{22} & 0\\ 0 & 0 & \eta_{33}\end{bmatrix},\quad q=\begin{bmatrix}0\\0\\q_3\end{bmatrix},\quad p=\begin{bmatrix}0\\0\\p_3\end{bmatrix}, \tag{3a}$$

$$S=\begin{bmatrix}S_{11} & S_{12} & S_{13} & 0 & 0 & 0\\ S_{12} & S_{22} & S_{23} & 0 & 0 & 0\\ S_{13} & S_{23} & S_{33} & 0 & 0 & 0\\ 0 & 0 & 0 & S_{44} & 0 & 0\\ 0 & 0 & 0 & 0 & S_{55} & 0\\ 0 & 0 & 0 & 0 & 0 & S_{66}\end{bmatrix},\quad d^T=\begin{bmatrix}0 & 0 & d_{31}\\ 0 & 0 & d_{32}\\ 0 & 0 & d_{33}\\ 0 & d_{24} & 0\\ d_{15} & 0 & 0\\ 0 & 0 & 0\end{bmatrix},\quad \alpha=\begin{bmatrix}\alpha_1\\ \alpha_2\\ \alpha_3\\ 0\\ 0\\ 0\end{bmatrix} \tag{3b}$$

Denoting differentiation by a subscript comma, components of strain and electric field in Cartesian coordinates are related to displacement components u, v, w along axes x, y, z and electrical potential ϕ by

$$\varepsilon_x=u_{,x},\ \varepsilon_y=0,\ \varepsilon_z=w_{,z},\ \gamma_{yz}=v_{,z},\ \gamma_{zx}=w_{,x}+u_{,z},\ \gamma_{xy}=v_{,x};\ E_x=-\phi_{,x},\ E_y=0,\ E_z=-\phi_{,z}. \tag{4}$$

Consider kth layer whose orientation of the principal material axes x_1 and x_2 is at an angle θ with respect to the axes x and y. Using Eqs. (1)-(4), the constitutive equations for the components with respect to the axes x, y, z, can be written as

$$u_{,x}=\bar{S}_{11}\sigma_x+\bar{S}_{12}\sigma_y+\bar{S}_{13}\sigma_z+\bar{S}_{16}\tau_{xy}-\bar{d}_{31}\phi_{,z}+\bar{\alpha}_1T, \tag{5}$$

$$0=\bar{S}_{12}\sigma_x+\bar{S}_{22}\sigma_y+\bar{S}_{23}\sigma_z+\bar{S}_{26}\tau_{xy}-\bar{d}_{32}\phi_{,z}+\bar{\alpha}_2T, \tag{6}$$

$$w_{,z}=\bar{S}_{13}\sigma_x+\bar{S}_{23}\sigma_y+\bar{S}_{33}\sigma_z+\bar{S}_{36}\tau_{xy}-\bar{d}_{33}\phi_{,z}+\bar{\alpha}_3T, \tag{7}$$

$$v_{,z}=\bar{S}_{44}\tau_{yz}+\bar{S}_{45}\tau_{zx}-\bar{d}_{14}\phi_{,x}, \tag{8}$$

$$w_{,x}+u_{,z}=\bar{S}_{45}\tau_{yz}+\bar{S}_{55}\tau_{zx}-\bar{d}_{15}\phi_{,x}, \tag{9}$$

$$v_{,x}=\bar{S}_{16}\sigma_x+\bar{S}_{26}\sigma_y+\bar{S}_{36}\sigma_z+\bar{S}_{66}\tau_{xy}-\bar{d}_{36}\phi_{,z}+\bar{\alpha}_6T, \tag{10}$$

$$D_x=\bar{d}_{14}\tau_{yz}+\bar{d}_{15}\tau_{zx}-\bar{\varepsilon}_{11}\phi_{,x}, \tag{11}$$

$$D_y=\bar{d}_{24}\tau_{yz}+\bar{d}_{25}\tau_{zx}-\bar{\varepsilon}_{12}\phi_{,x}, \tag{12}$$

$$D_z=\bar{d}_{31}\sigma_x+\bar{d}_{32}\sigma_y+\bar{d}_{33}\sigma_z+\bar{d}_{36}\tau_{xy}-\bar{\varepsilon}_{33}\phi_{,z}+\bar{q}_3T, \tag{13}$$

where

$$\bar{S}_{11}=c^4S_{11}+c^2s^2(2S_{12}+S_{66})+s^4S_{22},\ \bar{S}_{12}=c^2s^2(S_{11}+S_{22}-S_{66})+(c^4+s^4)S_{12},$$
$$\bar{S}_{13}=c^2S_{13}+s^2S_{23},\ \bar{S}_{16}=2cs[c^2S_{11}+(s^2-c^2)(\bar{S}_{12}+0.5S_{66})-s^2S_{22}],\ \bar{S}_{23}=s^2S_{13}+c^2S_{23},$$
$$\bar{S}_{22}=s^4S_{11}+c^2s^2(2S_{12}+S_{66})+c^4S_{22},\ \bar{S}_{26}=2cs[s^2S_{11}+(c^2-s^2)(S_{12}+0.5S_{66})-c^2S_{22}],$$
$$\bar{S}_{33}=S_{33},\ \bar{S}_{36}=2cs(S_{13}-S_{23}),\ \bar{S}_{44}=c^2S_{44}+s^2S_{55},\ \bar{S}_{45}=cs(S_{55}-S_{44}),$$
$$\bar{S}_{55}=s^2S_{44}+c^2S_{55},\ \bar{S}_{66}=4c^2s^2(S_{11}-2S_{12}+S_{22})+(c^2-s^2)^2S_{66};\quad c=\cos\theta,\quad s=\sin\theta,$$
$$\bar{d}_{31}=c^2d_{31}+s^2d_{32},\ \bar{d}_{32}=s^2d_{31}+c^2d_{32},\ \bar{d}_{33}=d_{33},\ \bar{d}_{36}=2cs(d_{31}-d_{32}),\ \bar{q}_3=q_3,$$

$$\bar{d}_{14}=\bar{d}_{25}=cs(d_{15}-d_{24}),\ \bar{d}_{24}=c^2d_{24}+s^2d_{15},\ \bar{d}_{15}=s^2d_{24}+c^2d_{15},$$
$$\bar{\alpha}_1=c^2\alpha_1+s^2\alpha_2,\ \bar{\alpha}_2=s^2\alpha_1+c^2\alpha_2,\ \bar{\alpha}_3=\alpha_3,\ \bar{\alpha}_6=2cs(\alpha_1-\alpha_2),$$
$$\bar{\varepsilon}_{11}=c^2\varepsilon_{11}+s^2\varepsilon_{22},\ \bar{\varepsilon}_{12}=cs(\varepsilon_{11}-\varepsilon_{22}),\ \bar{\varepsilon}_{22}=s^2\varepsilon_{11}+c^2\varepsilon_{22},\ \bar{\varepsilon}_{33}=\varepsilon_{33}. \tag{14}$$

Let k_i's be the thermal conductivity coefficients in the principal directions x_i of the material. The equations of thermal, force and charge equilibrium without heat source, body force and charge source are

$$\bar{k}_x T_{,xx}+\bar{k}_z T_{,zz}=0, \tag{15}$$

$$\sigma_{x,x}+\tau_{zx,z}=0,\ \tau_{xy,x}+\tau_{yz,z}=0,\ \tau_{zx,x}+\sigma_{z,z}=0,\ D_{x,x}+D_{z,z}=0, \tag{16}$$

with $\bar{k}_x=c^2k_1+s^2k_2$, $\bar{k}_z=k_3$. We introduce dimensionless coordinates ξ and $\zeta^{(k)}$ for the kth layer as:

$$\xi=x/a\ ,\quad \zeta^{(k)}=(z+h/2-\sum_{i=1}^{k-1}t^{(i)})/t^{(k)}. \tag{17}$$

Let the prescribed pressure, ambient temperature and ϕ or D_z at the lateral surfaces at $z=z_j$ be $P_j(\xi)$, $T_j(\xi)$, $\phi_j(\xi)$ or $D_j(\xi)$. Let the number of applied potential differences for actuation be L_p with the ith one $V_i(\xi)$ being applied between the interfaces l_i and m_i with $l_i<m_i$, and the number of interfaces with prescribed potentials be L_a with the qth one being $\Phi_q(\xi)$ for the interface n_q. Thus

at $\xi=0,\ 1$; $\qquad w=0,\ \sigma_x=0,\ \tau_{xy}=0,\ \phi=0,\ T=0;$ (18)

at $z=z_j$; $\qquad \sigma_z=-P_j(\xi),\ \tau_{yz}=0,\ \tau_{zx}=0,\ \phi=\phi_j(\xi)$ *or* $D_z=D_j(\xi),\quad j=1,\ 2;$ (19a)

and at $z=-h/2$, ; $-\bar{k}_z T_{,z}+h_1T=h_1T_1(\xi)$, $\qquad z=h/2$: $\bar{k}_z T_{,z}+h_2T=h_2T_2(\xi)$. (20)

h_1 and h_2 are the surface heat transfer coefficients at the surfaces of the plate. The special case $h_1=h_2=\infty$ corresponds to the temperature of the surfaces being prescribed as $T_1(\xi)$ and $T_2(\xi)$. The conditions of prescribed potential difference and prescribed potentials of interfaces are expressed as

$$[\phi|_{\zeta=1}]^{(m_i)}-[\phi|_{\zeta=0}]^{(l_i+1)}=V_i(\xi),\quad i=1,\ \cdots,\ L_p;\ [\Phi|_{\zeta=1}]^{(n_q)}=\Phi_q(\xi),\quad q=1,\ \cdots,\ L_a. \tag{21}$$

The equilibrium and compatibility conditions at the interface between adjacent layers are:

$$[T|_{\zeta=1}]^{(k)}=[T|_{\zeta=0}]^{(k+1)},\ [\bar{k}_2T_{,\zeta}|_{\zeta=1}/t]^{(k)}=[\bar{k}_zT_{,\zeta}|_{\zeta=0}/t]^{(k+1)},\qquad k=1,\ \cdots,\ L-1; \tag{22}$$

$$[(u,v,w,\sigma_z,\tau_{yz},\tau_{zx},\phi,D_z)|_{\zeta=1}]^{(k)}=[(u,v,w,\sigma_z,\tau_{yz},\tau_{zx},\phi,D_z)|_{\zeta=0}]^{(k+1)},\qquad k=1,\ \cdots,\ L-1. \tag{23a}$$

The applied potential difference V_i induces extraneous surface charge density, say $\sigma_i(\xi)$, and $-\sigma_i(\xi)$ at the interfaces m_i and l_i. The potential Φ_q induces an extraneous surface charge density, say $\tau_q(\xi)$ at the interface n_q. Hence the conditions (23a) for continuity of D_z need to be modified. For $i=1,\ \cdots,\ L_p$:

if $m_i\neq$L, then $\qquad D_z^{(m_i)}|_{\zeta=1}=D_z^{(m_i+1)}|_{\zeta=0}-\sigma_i(\xi),$ (23b)

if $l_i\neq0$, then $\qquad D_z^{(l_i)}|_{\zeta=1}=D_z^{(l_i+1)}|_{\zeta=0}+\sigma_i(\xi),$ (23c)

if $m_i=L$ and D_2 is prescribed, then Eq. (19a) for D_z is modified as $[D_z|_{\zeta=1}]^{(L)}=D_2+\sigma_i,$ (19b)

if l_i=0 and D_1 is prescribed, then Eq. (19a) for D_z is modified as $[D_z|_{\zeta=0}]^{(1)} = D_1 - \sigma_i$, (19c)

$$[D_z|_{\zeta=1}]^{(n_q)} = [D_z|_{\zeta=0}]^{(n_q+1)} - \tau_q(\xi), \quad q=1, \cdots, L_a. \tag{23d}$$

3. General solution

The solution for the kth layer, satisfying boundary conditions (18), is taken in the form of Fourier series:

$$(w, \sigma_x, \sigma_y, \sigma_z, \tau_{xy}, \phi, D_z, T) = \sum_{n=1}^{\infty} (w_n, \sigma_{x_n}, \sigma_{y_n}, \sigma_{z_n}, \tau_{xy_n}, \phi_n, D_{z_n}, T_n) \sin n\pi\xi,$$

$$(u, v, \tau_{yz}, \tau_{zx}, D_x, D_y) = \sum_{n=1}^{\infty} (u_n, v_n, \tau_{yz_n}, \tau_{zx_n}, D_{x_n}, D_{y_n}) \cos n\pi\xi; \tag{24}$$

$$(P_i, \phi_i, D_i, T_i, V_i, \Phi_i, \sigma_i, \tau_i) = \sum_{n=1}^{\infty} (P_{i_n}, \phi_{i_n}, D_{i_n}, T_{i_n}, V_{i_n}, \Phi_{i_n}, \sigma_{i_n}, \tau_{i_n}) \sin n\pi\xi. \tag{25}$$

Substituting the expansion of T from Eq. (24) into the heat conduction Eq. (15) yields

$$T_{n,\zeta\zeta} - \mu_n^2 T_n = 0, \text{ with } \mu_n = \bar{n}t(\bar{k}_x/\bar{k}_z)^{1/2}, \quad \bar{n} = n\pi/a. \tag{26}$$

Using the expansions (24), the thirteen constitutive and equilibrium Eqs. (5)-(13) and (16) are transformed into eight first order differential equations in terms of u_n, v_n, w_n, σ_{z_n}, τ_{yz_n}, τ_{zx_n}, ϕ_n, D_{z_n} and five algebraic equations for σ_{x_n}, σ_{y_n}, τ_{xy_n}, D_{x_n}, D_{y_n}:

$$D_{x_n} = \bar{d}_{14}\tau_{yz_n} + \bar{d}_{15}\tau_{zx_n} - \bar{n}\,\bar{\varepsilon}_{11}\phi_n, \quad D_{yn} = \bar{d}_{24}\tau_{yz_n} + \bar{d}_{25}\tau_{zx_n} - \bar{n}\,\bar{\varepsilon}_{12}\phi_n, \tag{27}$$

$$\sigma_{x_n} = \bar{n}p_{11}u_n + \bar{n}p_{12}v_n + p_{14}\sigma_{z_n} + p_{18}D_{z_n} + t_1T_n, \tag{28}$$

$$\sigma_{y_n} = \bar{n}p_{21}u_n + \bar{n}p_{22}v_n + p_{24}\sigma_{z_n} + p_{28}D_{z_n} + t_2T_n, \tag{29}$$

$$\tau_{xyn} = \bar{n}p_{61}u_n + \bar{n}p_{62}v_n + p_{64}\sigma_{zn} + p_{68}D_{zn} + t_6T_n, \tag{30}$$

with $p_{i1} = -\hat{S}_{i1}, p_{i2} = -\hat{S}_{i6}, p_{i4} = -(\hat{S}_{i1}\bar{S}'_{13} + \hat{S}_{i2}\bar{S}'_{23} + \hat{S}_{i6}\bar{S}'_{36}), p_{i8} = -(\hat{S}_{i1}\bar{d}'_{31} + \hat{S}_{i2}\bar{d}'_{32} + \hat{S}_{i6}\bar{d}'_{36}),$

$t_i = -(\hat{S}_{i1}\bar{\alpha}'_1 + \hat{S}_{i2}\bar{\alpha}'_2 + \hat{S}_{i6}\bar{\alpha}'_6), \ \bar{d}'_{ij} = \bar{d}_{ij}/\bar{\varepsilon}_{33}, \ \bar{\alpha}'_i = \bar{\alpha}'_i - \bar{d}'_{3i}\bar{q}_3, \ \bar{S}'_{ij} = \bar{S}_{ij} - \bar{d}_{3i}\bar{d}'_{3j}$,

$$\begin{bmatrix} \hat{S}_{11} & \hat{S}_{12} & \hat{S}_{16} \\ \hat{S}_{12} & \hat{S}_{22} & \hat{S}_{26} \\ \hat{S}_{16} & \hat{S}_{26} & \hat{S}_{66} \end{bmatrix} = \begin{bmatrix} \bar{S}'_{11} & \bar{S}'_{12} & \bar{S}'_{16} \\ \bar{S}'_{12} & \bar{S}'_{22} & \bar{S}'_{26} \\ \bar{S}'_{16} & \bar{S}'_{26} & \bar{S}'_{66} \end{bmatrix}^{-1}, \tag{31}$$

and

$$X_{n,z} = AX_n + QT_n, \tag{32}$$

where $X_n = [u_n \ v_n \ w_n \ \sigma_{zn} \ \tau_{yzn} \ \tau_{zxn} \ \phi_n \ D_{zn}]^T$.

The nonzero elements of matrix A and vector Q are given by:

$$a_{13} = -\bar{n}, \ a_{15} = \bar{S}_{45}, \ a_{16} = \bar{S}_{55}, \ a_{17} = -\bar{n}\,\bar{d}_{15}, \ a_{25} = \bar{S}_{44}, \ a_{26} = \bar{S}_{45}, \ a_{27} = -\bar{n}\,\bar{d}_{14},$$
$$a_{31} = \bar{n}(\bar{S}'_{13}p_{11} + \bar{S}'_{23}p_{21} + \bar{S}'_{36}p_{61}), \ a_{32} = \bar{n}(\bar{S}'_{13}p_{12} + \bar{S}'_{23}p_{22} + \bar{S}'_{36}p_{62}), \ a_{46} = \bar{n},$$
$$a_{34} = \bar{S}'_{13}p_{14} + \bar{S}'_{23}p_{24} + \bar{S}'_{36}p_{64} + \bar{S}'_{33}, \ a_{38} = \bar{S}'_{13}p_{18} + \bar{S}'_{23}p_{28} + \bar{S}'_{36}p_{68} + d'_{33}, \ a_{51} = -\bar{n}^2 p_{61},$$

$$a_{52}=-\bar{n}^2 p_{62},\quad a_{54}=-\bar{n}\,p_{64},\quad a_{58}=-\bar{n}\,p_{68},\quad a_{61}=-\bar{n}^2 p_{11},\quad a_{62}=-\bar{n}^2 p_{12},\quad a_{64}=-\bar{n}\,p_{14},$$
$$a_{68}=-\bar{n}p_{18},\quad a_{71}=\bar{n}(\bar{d}'_{31}p_{11}+\bar{d}'_{32}p_{21}+\bar{d}'_{36}p_{61}),\quad a_{72}=\bar{n}\,(\bar{d}'_{31}p_{12}+\bar{d}'_{32}p_{22}+\bar{d}'_{36}p_{62}),$$
$$a_{74}=\bar{d}'_{31}p_{14}+\bar{d}'_{32}p_{24}+\bar{d}'_{36}p_{64}+\bar{d}'_{33},\quad a_{78}=\bar{d}'_{31}p_{28}+\bar{d}'_{32}p_{28}+\bar{d}'_{36}p_{68}-1/\bar{\varepsilon}_{33},$$
$$a_{85}=\bar{n}\,\bar{d}_{14},\quad a_{86}=\bar{n}\,\bar{d}_{15},\quad a_{87}=-\bar{n}^2\bar{\varepsilon}_{11}$$
$$Q_3=\bar{S}'_{13}t_1+\bar{S}'_{23}t_2+\bar{S}'_{36}t_6+\bar{\alpha}'_3,\quad Q_5=-\bar{n}t_6,\quad Q_6=-\bar{n}t_1,\quad Q_7=\bar{d}'_{31}t_1+\bar{d}'_{32}t_2+\bar{d}'_{36}t_6+\bar{q}_3/\bar{\varepsilon}_{33}. \quad (33)$$

With ρ_1, $\rho_2=\mp\mu_n$, the general solution of Eq. (2.26), in terms of two arbitrary constants A_1^n and A_2^n is

$$T_n=\sum_{i=1}^{2} e^{\rho i\zeta}A_i^n. \quad (34)$$

The general solution of Eq. (32) is obtained as the sum of the complementary X_n^c and X_n^p with $X_n^c=e^{\lambda\zeta}Y$. Substituting X_n^c into the homogeneous part of Eq. (32) yields

$$AY=\lambda Y. \quad (35)$$

Hence the exponent λ and Y are eigenvalue and eigenvector pair of real matrix A. These are obtained by QR algorithm after first reducing to Heissenberg form. The eigenvalues of A are either real or occur in complex conjugate pairs. The complementary solution for pair of eigenvalues λ_1, $\lambda_2=\alpha\pm i\beta$ with complex eigenvector Y_1 corresponding to λ_1, can be expressed in terms of two real constants C_1^n and C_2^n as

$$X_n^c(\zeta)=F_1^n(\zeta)C_1^n+F_2^n(\zeta)C_2^n, \quad (36a)$$

with $F_1^n(\zeta)=e^{\alpha\zeta}[\cos(\beta\zeta)R(Y_1)-\sin(\beta\zeta)F(Y_1)]$, $F_2^n(\zeta)=e^{\alpha\zeta}[\sin(\beta\zeta)R(Y_1)+\cos(\beta\zeta)F(Y_1)]$. (36b)

R and F indicate real and imaginary parts of a complex number. The complementary solution for distinct real eigenvalue, say $\lambda_3=p$ with eigenvector Y_3, in terms of real constant C_3^n, is

$$X_n^c(\zeta)=F_3^n(\zeta)C_3^n \quad \text{with} \quad F_3^n(\zeta)=e^{p\zeta}Y_3. \quad (37)$$

Thus the complete complementary solution X_n^c can be expressed in terms of eight real constants C_j^n as

$$X_n^c(\zeta)=\sum_{j=1}^{8} F_j^n(\zeta)C_j^n, \quad (38)$$

where the functional form of $F_j^n(\zeta)$ is given by Eqs. (36) or (37) as per the nature of λ_j. Substituting T_n from Eq. (34) into Eq. (32), the particular solution X_n^p of Eq. (32) can be obtained as

$$X_n^p=\sum_{i=1}^{2} G_i^n(\zeta)A_i^n, \quad \text{where} \quad G_i^n=-[A(\rho_i)-\rho_i I/t]^{-1}Qe^{\rho i\zeta}. \quad (39)$$

Thus the general solution of Eq. (32) is

$$X_n=\sum_{j=1}^{8} F_j^n(\zeta)C_j^n+\sum_{i=1}^{2} G_i^n(\zeta)A_i^n. \quad (40)$$

The $2L$ constants A_j^n for all L layers in the thermal solution are determined from the $2L$ thermal boundary and interface conditions (20) and (22). The $8L$ constants C_j^n for L layers

and L_p+L_a unknown charge densities σ_{i_n} and τ_{q_n} are obtained from the $8L+L_p+L_a$ conditions (19), (21) and (23). The various entities are then completely determined from (34), (40) and (27)-(30). The numerical solution is obtained by taking finite number of terms, say N, in the expansions (24).

The two dimensional uncoupled classical laminate theory (CLT), presented by Tauchert (1992), and the first order shear deformation theory (FSDT), presented by Jonnalagadda *et al.* (1994), for given thermoelectric field are assessed by comparison with the present plane strain solution. In the 2D theories, the temperature distribution has been taken as the one obtained by the exact solution of the heat conduction equation and the electric potential ϕ is assumed to vary linearly across the thickness of the actuated piezoelectric layer and zero elsewhere. Navier-type solutions are obtained for the 2D theories.

4. Numerical results and discussion

Results are presented for seven-layered hybrid plates made of an elastic substrate of graphite-epoxy, with a distributed piezoceramic layer of PZT-5A having thickness $h/10$, bonded to its top surface. The substrate is a six-layered, angle-ply laminate with the orientations of the fibres of the plies being $[\theta^\circ/-\theta^\circ/\theta^\circ]_s$ relative to x-direction. All plies of the substrate have equal thickness. The material properties of the graphite-epoxy composite are selected as in Xu *et al.* (1995):

$(Y_L, Y_T, G_{LT}, G_{TT}) = (181, 10.3, 7.17, 2.87)$ GPa, $(\nu_{LT}, \nu_{TT}) = (0.28, 0.33)$, $(k_L, k_T) = (1.5, 0.5)$ $\mathrm{Wm^{-1}K^{-1}}$, $(\alpha_L, \alpha_T) = (0.02, 22.5) \times 10^{-6}\ \mathrm{K^{-1}}$, $p_3=0$, $\eta_L=\eta_T=1.53\times 10^{-8}$ F/m, $d_{ij}=0$

where L and T are directions parallel and transverse to the fibres. Y_i, G_{ij}, ν_{ij}, η_i, d_{ij}, p_3 are Young's moduli, shear moduli, Poisson's ratios, permittivity constants, piezoelectric strain constants and pyroelectric constant, respectively. The properties of PZT-5A are taken as in Xu *et al.* (1995):

$(Y_1, Y_2, Y_3, G_{12}, G_{23}, G_{31}) = (61.0, 61.0, 53.2, 22.6, 21.1, 21.1)$ GPa, $(\nu_{12}, \nu_{23}, \nu_{13}) = (0.35, 0.38, 0.38)$, $(\alpha_1, \alpha_2, \alpha_3) = (1.5, 1.5, 2.0) \times 10^{-6}\ \mathrm{K^{-1}}$, $k_x = k_y = k_z = 1.8\ \mathrm{Wm^{-1}K^{-1}}$, $p_3 = 0.0007\ \mathrm{Cm^{-2}K^{-1}}$, $(\eta_1, \eta_2, \eta_3) = (1.53, 1.53, 1.50) \times 10^{-8}$ F/m, $(d_{31}, d_{32}, d_{33}, d_{24}, d_{15}) = (-171, -171, 374, 584, 584) \times 10^{-12}\ \mathrm{m/V}$.

The response under the following sinusoidal thermoelectromechanical loads is determined:

1. $\phi_1=\phi_2=0$, $T_1=T_2=0$, $P_1=0$, $P_2=p_0 \sin \pi\xi$,
2. $\phi_1=\phi_2=0$, $T_1=0$, $T_2=T_0 \sin \pi\xi$, $P_1=P_2=0$,
3. $\phi_1=0$, $\phi_2=\phi_0 \sin \pi\xi$, $T_1=T_2=0$, $P_1=P_2=0$.

T_i's are the prescribed temperatures of the surfaces of the plate. The interface of the piezoelectric layer with the substrate is grounded. The results for the three cases are nondimensionalised as follows with $S=a/h$, $d_T=374\times 10^{-12}\ \mathrm{CN^{-1}}$, $\alpha_T=22.5\times 10^{-6}\ \mathrm{K^{-1}}$, $E_T=10.3$ GPa:

1. $(\bar{w}, \bar{u}) = 100(w, u) E_T/hS^3 p_0, (\bar{\sigma}_x, \bar{\sigma}_y, \bar{\tau}_{xy}) = 10(\sigma_x, \sigma_y, \tau_{xy})/S^2 p_0, (\bar{\sigma}_z, \bar{\tau}_{yz}, \bar{\tau}_{zx}) = (S\sigma_z, 10\tau_{yz}, \tau_{zx})/Sp_0, \bar{\phi} = \phi d_T E_T/hS^2 p_0, \bar{D}_z = D_z/d_T S^2 p_0$;

2. $(\hat{w}, \hat{u}) = 1000(w, u)/h\,\alpha_T S^2 T_0$, $(\hat{\sigma}_x, \hat{\sigma}_y, \hat{\tau}_{xy}, \hat{\sigma}_z, \hat{\tau}_{yz}, \hat{\tau}_{zx}) = 10(\sigma_x, \sigma_y, \tau_{xy}, S^2\sigma_z, S\,\tau_{yz}, S\,\tau_{zx})/\alpha_T E_T T_0$, $\hat{\phi} = \phi d_T/h\,\alpha_T S T_0$, $\hat{D}_z = D_z/E_T d_T \alpha_T T_0$;

3. $(\tilde{w}, \tilde{u}) = 10(w, Su)/S^3 d_T \phi_0$, $(\tilde{\sigma}_x, \tilde{\sigma}_y, \tilde{\tau}_{xy}) = 0.1(\sigma_x, \sigma_y, \tau_{xy})h/E_T d_T \phi_0$, $\tilde{\phi} = \phi/\phi_0$, $\tilde{D}_z = 0.01\, D_z h/E_T d_T^2 \phi_0$; $(\tilde{\sigma}_z, \tilde{\tau}_{yz}, \tilde{\tau}_{zx}) = (S\,\sigma_z, \tau_{yz}, \tau_{zx})Sh/E_T d_T \phi_0$.

Table 1 Effect of S for hybrid plate under pressure load of case 1

	S	0°	15°	30°	45°	60°	75°	90°
$\bar{u}(0, -0.5h)$	4	−1.438	−1.654	−2.369	−4.024	−7.721	−12.81	−14.36
	10	−1.268	−1.430	−2.025	−3.542	−7.133	−12.16	−13.66
	100	−1.229	−1.381	−1.952	−3.442	−7.012	−12.03	−13.52
$\bar{w}(0.5a, 0)$	4	−1.919	−2.129	−2.771	−3.965	−5.994	−8.292	−8.969
	10	−1.009	−1.123	−1.524	−2.430	−4.209	−6.301	−6.887
	100	−0.8331	−0.9287	−1.282	−2.133	−3.866	−5.920	−6.489
$\bar{\sigma}_x(0.5a, -0.5h)$	4	7.974	7.721	7.147	6.253	5.234	4.639	4.531
	10	7.031	6.892	6.532	5.861	4.954	4.406	4.312
	100	6.815	6.705	6.402	5.783	4.896	4.358	4.267
$\bar{\sigma}_x(0.5a, 0.4h^-)$	4	−6.831	−6.609	−5.824	−4.515	−2.894	−1.749	−1.520
	10	−6.321	−6.201	−5.682	−4.596	−2.964	−1.752	−1.519
	100	−6.223	−6.123	−5.666	−4.625	−2.982	−1.753	−1.519
$\bar{\sigma}_x(0.5a, 0.5h)$	4	−4.328	−4.744	−6.059	−8.513	−12.14	−15.10	−15.77
	10	−3.199	−3.535	−4.728	−7.280	−11.29	−14.44	−15.10
	100	−2.993	−3.313	−4.476	−7.046	−11.14	−14.32	−14.98
$\bar{\sigma}_y(0.5a, -0.5h)$	4	0.1271	0.6010	2.066	4.493	6.740	4.613	1.269
	10	0.1120	0.5441	1.922	4.312	6.546	4.403	1.207
	100	0.1086	0.5310	1.892	4.278	6.506	4.358	1.195
$\bar{\sigma}_y(0.5a, 0.4h^-)$	4	−0.3112	−0.7123	−1.862	−3.429	−4.118	−2.233	−0.5892
	10	−0.1332	−0.5242	−1.713	−3.472	−4.268	−2.162	−0.4515
	100	−0.0995	−0.4887	−1.690	−3.496	−4.308	−2.149	−0.4256
$\bar{\sigma}_y(0.5a, 0.5h)$	4	−1.843	−1.998	−2.486	−3.398	−4.759	−5.898	−6.162
	10	−1.203	−1.326	−1.762	−2.696	−4.180	−5.376	−5.634
	100	−1.086	−1.202	−1.625	−2.563	−4.074	−5.282	−5.539
$\bar{\sigma}_z(0.5a, 0)$	4	−0.5300	−0.5264	−0.5130	−0.4840	−0.4393	−0.4061	−0.3996
	10	−0.5410	−0.5368	−0.5215	−0.4883	−0.4377	−0.4019	−0.3952
	100	−0.5427	−0.5383	−0.5228	−0.4889	−0.4371	−0.4009	−0.3942
$\bar{\tau}_{yz}(0, -0.35h)$	4	0.0	−0.6092	−1.173	−1.620	−1.574	−0.6137	0.0
	10	0.0	−0.6296	−1.238	−1.708	−1.612	−0.6030	0.0
	100	0.0	−0.6318	−1.250	−1.727	−1.619	−0.6001	0.0
$\bar{\tau}_{zx}(0, 0)$	4	−4.738	−4.750	−4.738	−4.604	−4.360	−4.193	−4.162
	10	−4.964	−4.942	−4.865	−4.681	−4.398	−4.209	−4.176
	100	−5.013	−4.983	−4.891	−4.695	−4.404	−4.212	−4.178
$\bar{\tau}_{xy}(0.5a, -0.5h)$	4	0.0	1.777	3.403	4.499	4.109	1.542	0.0
	10	0.0	1.632	3.196	4.348	4.013	1.474	0.0
	100	0.0	1.598	3.152	4.321	3.993	1.459	0.0
$\bar{\phi}(0.5a, 0.45h)$	4	−0.8316	−0.9176	−1.179	−1.667	−2.503	−3.463	−3.747
	10	−0.4221	−0.4697	−0.6366	−1.015	−1.759	−2.637	−2.883
	100	−0.3498	−0.3900	−0.5382	−0.8958	−1.624	−2.486	−2.725
$\bar{D}_z(0.5a, 0.45h)$	4	0.1665	0.1872	0.2529	0.3756	0.5504	0.6763	0.7006
	10	0.1642	0.1822	0.2459	0.3810	0.5844	0.7267	0.7530
	100	0.1639	0.1813	0.2443	0.3817	0.5911	0.7366	0.7632

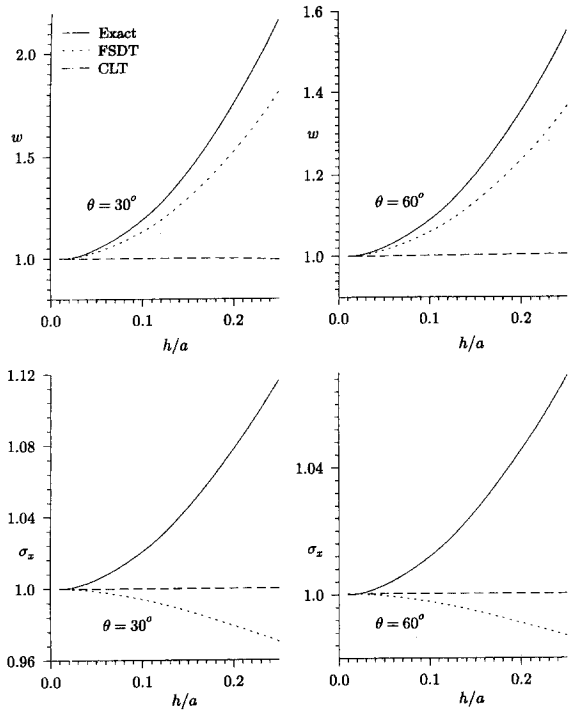

Fig. 2 Effect of h/a on $w(0.5a, 0)$ and $\sigma_x(0.5a, -0.5h)$ for load case 1

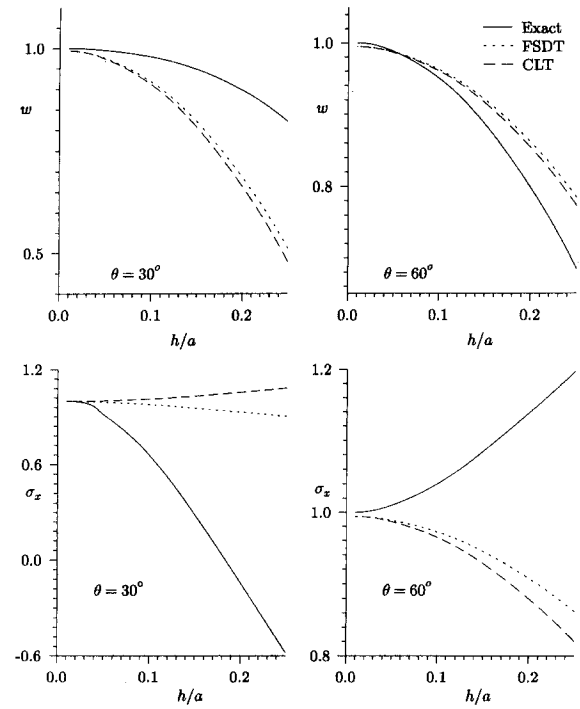

Fig. 3 Effect of h/a on $w(0.5a, 0)$ and $\sigma_x(0.5a, -0.5h)$ for load case 2

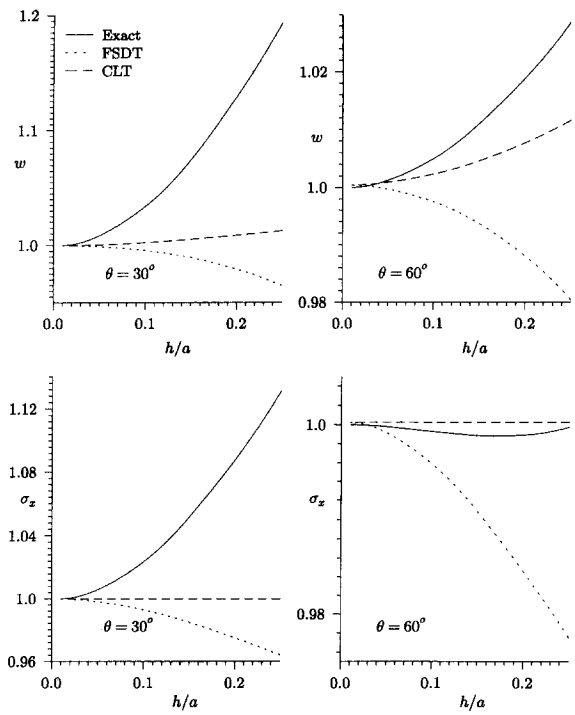

Fig. 4 Effect of h/a on $w(0.5a, 0)$ and $\sigma_x(0.5a, 0.4h)$ for load case 3

The response of the hybrid plates to pressure load of case 1, obtained using generalised plane strain solution, is presented in Table 1. The values of the displacements and stresses, at points where they are high, are given for three values of S and seven values of θ. It is observed that the ply-angle θ has a significant effect on all the displacement and stress

Table 2 Effect of S for hybrid plate under thermal load of case 2

	S	0°	15°	30°	45°	60°	75°	90°
$\hat{u}(0, -0.5h)$	4	−3.658	−4.380	−5.486	−10.27	−33.79	−87.66	−109.3
	10	0.6661	0.0162	−0.9965	−5.904	−31.77	−90.78	−113.9
	100	1.873	1.222	0.1592	−4.878	−31.30	−91.38	−114.8
$\hat{w}(0.5a, 0)$	4	2.917	3.450	5.268	8.150	7.681	−4.065	−9.595
	10	3.654	4.214	6.282	10.09	10.65	−1.566	−7.308
	100	3.740	4.304	6.417	10.43	11.22	−1.088	−6.872
$\hat{\sigma}_x(0.5a, -0.5h)$	4	2.028	1.353	0.8212	0.8587	1.811	3.062	3.448
	10	−0.3694	−0.9071	−0.9261	−0.1350	1.574	3.166	3.594
	100	−1.039	−1.536	−1.413	−0.4017	1.514	3.185	3.622
$\hat{\sigma}_x(0.5a, 0.4h^-)$	4	5.327	3.839	1.352	−1.453	−4.341	−6.302	−6.825
	10	2.673	1.676	0.3216	−1.589	−4.249	−6.228	−6.751
	100	1.946	1.081	0.0416	−1.622	−4.229	−6.213	−6.737
$\hat{\sigma}_x(0.5a, 0.5h)$	4	−1.713	−1.169	0.3915	3.507	8.435	12.29	13.30
	10	−3.872	−3.351	−1.724	1.911	7.811	12.16	13.22
	100	−4.396	−3.878	−2.230	1.536	7.672	12.13	13.20
$\hat{\sigma}_y(0.5a, -0.5h)$	4	0.0323	0.0807	0.1698	0.4097	1.654	2.171	0.9654
	10	−0.0059	−0.1025	−0.3670	−0.3933	1.205	2.201	1.006
	100	−0.0166	−0.1538	−0.5191	−0.6150	1.088	2.205	1.014
$\hat{\sigma}_y(0.5a, 0.4h^-)$	4	−9.455	−8.613	−6.318	−3.093	−0.6544	−1.330	−2.073
	10	−9.630	−8.896	−6.664	−3.122	−0.4251	−1.267	−2.044
	100	−9.669	−8.967	−6.753	−3.125	−0.3691	−1.255	−2.038
$\hat{\sigma}_y(0.5a, 0.5h)$	4	−4.881	−4.683	−4.114	−2.992	−1.253	0.0546	0.3847
	10	−5.586	−5.400	−4.819	−3.526	−1.455	0.0124	0.3579
	100	−5.759	−5.575	−4.989	−3.652	−1.501	0.0025	0.3512
$\hat{\sigma}_z(0.5a, 0.1h)$	4	−0.3558	−0.2710	−0.2577	−0.5538	−1.293	−2.021	−2.231
	10	0.4497	0.4577	0.2834	−0.2601	−1.258	−2.102	−2.327
	100	0.6775	0.6637	0.4318	−0.1843	−1.248	−2.118	−2.346
$\hat{\tau}_{yz}(0, 0.25h)$	4	0.0	0.8778	1.737	2.254	1.914	0.7469	0.0
	10	0.0	0.9219	1.918	2.535	2.079	0.7635	0.0
	100	0.0	0.9222	1.953	2.603	2.118	0.7669	0.0
$\hat{\tau}_{zx}(0, 0.25h)$	4	0.7059	0.3151	0.0129	0.1122	0.6888	1.331	1.516
	10	−0.2010	−0.4720	−0.5076	−0.1358	0.6739	1.416	1.615
	100	−0.4626	−0.7001	−0.6526	−0.1983	0.6688	1.433	1.634
$\hat{\tau}_{xy}(0.5a, 0.4h^-)$	4	0.0	3.150	5.473	6.453	5.226	2.258	0.0
	10	0.0	2.712	5.123	6.546	5.418	2.289	0.0
	100	0.0	2.587	5.023	6.570	5.464	2.295	0.0
$\hat{\phi}(0.5a, 0.45h)$	4	−0.2988	−0.2919	−0.2715	−0.2424	−0.2294	−0.2690	−0.2883
	10	−0.2591	−0.2559	−0.2450	−0.2261	−0.2212	−0.2709	−0.2943
	100	−0.2514	−0.2490	−0.2401	−0.2232	−0.2199	−0.2715	−0.2958
$\hat{D}_z(0.5a, 0.45h)$	4	8.280	8.250	8.166	7.991	7.694	7.432	7.358
	10	8.441	8.411	8.317	8.103	7.742	7.444	7.365
	100	8.478	8.448	8.351	8.129	7.752	7.447	7.366

components. However, the thickness parameter has a less pronounced effect on $\bar{\sigma}_z$, $\bar{\tau}_{yz}$, $\bar{\tau}_{zx}$, $\bar{D}_z$. The value of electric potential induced in the elastic substrate, not included for brevity, is found to be negligible. The comparison of CLT and FSDT solutions with the generalised plane strain solution is presented in Fig. 2. In Figs. 2-4, the entities plotted are normalised

Table 3 Effect of S for hybrid plate under potential load of case 3

	S	0°	15°	30°	45°	60°	75°	90°
$\tilde{u}(0, -0.5h)$	4	1.354	1.504	2.105	3.356	5.311	6.825	7.123
	10	1.568	1.700	2.285	3.595	5.644	7.164	7.452
	100	1.621	1.750	2.331	3.645	5.710	7.231	7.517
$\tilde{w}(0.5a, 0)$	4	1.997	2.216	2.915	4.221	6.081	7.418	7.675
	10	1.702	1.883	2.527	3.890	5.942	7.376	7.640
	100	1.640	1.814	2.444	3.818	5.912	7.367	7.633
$\tilde{\sigma}_x(0.5a, -0.5h)$	4	−0.7509	−0.7529	−0.6903	−0.5659	−0.3851	−0.2510	−0.2248
	10	−0.8695	−0.8854	−0.8260	−0.6694	−0.4293	−0.2646	−0.2352
	100	−0.8991	−0.9193	−0.8627	−0.6964	−0.4394	−0.2673	−0.2372
$\tilde{\sigma}_x(0.5a, 0.4h^-)$	4	2.121	1.961	1.630	1.207	0.7660	0.4985	0.4485
	10	1.754	1.659	1.476	1.174	0.7656	0.4944	0.4446
	100	1.672	1.590	1.442	1.169	0.7662	0.4936	0.4438
$\tilde{\sigma}_x(0.5a, 0.5h)$	4	−3.162	−3.048	−2.710	−2.103	−1.273	−0.7004	−0.5919
	10	−3.363	−3.269	−2.960	−2.321	−1.376	−0.7338	−0.6172
	100	−3.406	−3.316	−3.015	−2.369	−1.397	−0.7402	−0.6220
$\tilde{\sigma}_y(0.5a, -0.5h)$	4	−0.0120	−0.0604	−0.2040	−0.4191	−0.5315	−0.2806	−0.0629
	10	−0.0138	−0.0722	−0.2498	−0.5122	−0.6190	−0.3042	−0.0658
	100	−0.0143	−0.0752	−0.2623	−0.5369	−0.6398	−0.3091	−0.0664
$\tilde{\sigma}_y(0.5a, 0.4h^-)$	4	0.0371	0.1540	0.4665	0.8512	0.9678	0.4922	0.1263
	10	0.0285	0.1297	0.4296	0.8534	1.005	0.4995	0.1246
	100	0.0267	0.1242	0.4216	0.8559	1.015	0.5011	0.1243
$\tilde{\sigma}_y(0.5a, 0.5h)$	4	−3.810	−3.769	−3.648	−3.430	−3.132	−2.926	−2.886
	10	−3.878	−3.844	−3.733	−3.503	−3.163	−2.932	−2.890
	100	−3.892	−3.860	−3.752	−3.520	−3.170	−2.933	−2.891
$\tilde{\sigma}_z(0.5a, 0.1h)$	4	4.738	4.686	4.376	3.634	2.462	1.606	1.273
	10	5.619	5.533	5.113	4.155	2.693	1.693	1.512
	100	5.828	5.735	5.286	4.272	2.741	1.710	1.526
$\tilde{\tau}_{yz}(0, 0.25h)$	4	0.0	1.284	2.397	2.878	2.095	0.5768	0.0
	10	0.0	1.372	2.670	3.294	2.369	0.6245	0.0
	100	0.0	1.385	2.731	3.397	2.434	0.6346	0.0
$\tilde{\tau}_{zx}(0, 0.4h^-)$	4	−10.24	−9.904	−8.922	−7.169	−4.776	−3.131	−2.820
	10	−10.79	−10.51	−9.626	−7.788	−5.075	−3.237	−2.904
	100	−10.91	−10.65	−9.782	−7.925	−5.138	−3.258	−2.920
$\tilde{\tau}_{xy}(0.5a, 0.4h^-)$	4	0.0	0.4409	0.7580	0.8451	0.5867	0.1637	0.0
	10	0.0	0.3823	0.7091	0.8572	0.6153	0.1678	0.0
	100	0.0	0.3688	0.6986	0.8621	0.6225	0.1687	0.0
$\tilde{\phi}(0.5a, 0.45h)$	4	0.5006	0.5007	0.5009	0.5014	0.5022	0.5027	0.5028
	10	0.5007	0.5007	0.5010	0.5016	0.5024	0.5030	0.5031
	100	0.5007	0.5008	0.5010	0.5016	0.5025	0.5031	0.5032
$\tilde{D}_z(0.5a, 0.45h)$	4	−1.279	−1.286	−1.305	−1.340	−1.387	−1.419	−1.425
	10	−1.269	−1.274	−1.292	−1.328	−1.381	−1.417	−1.424
	100	−1.267	−1.272	−1.289	−1.325	−1.380	−1.417	−1.424

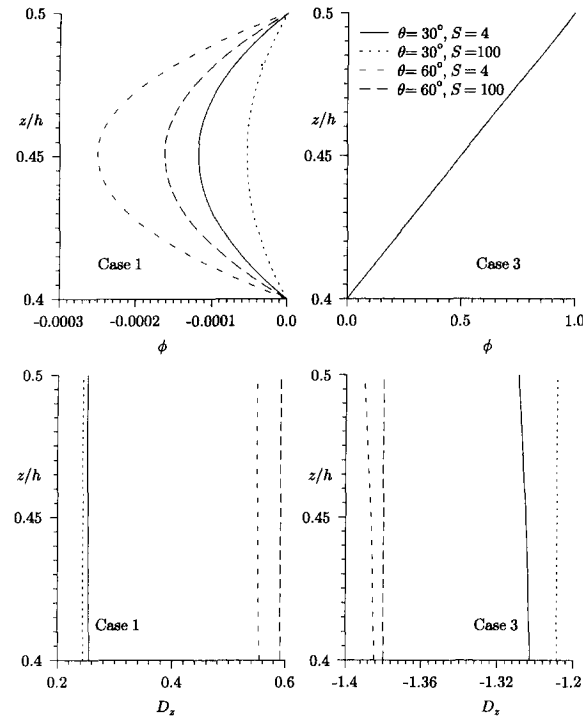

Fig. 5 Distributions of $\phi(0.5a, z)$ and $D_z(0.5a, z)$ across the piezoelectric layer for load cases 1 and 3

with respect to their values for the plane strain solution of a plate with $S=a/h=100$, e.g., the deflection w in these figures represents $w/[w$ for $S=100$ using plane strain solution]. It is observed from Fig. 2 that the values of σ_x obtained by FSDT and CLT solutions differ by less than 10% from the plane strain solution even for thick plates with $h/a=0.2$. The deflection w predicted by the 2D theories is in agreement with the plane strain solution for thin plate with $h/a=0.01$, but differ as the plate becomes thicker. The FSDT solution for deflection is a significant improvement over the CLT solution. The FSDT underestimates the deflection by less than 5% for plates with $h/a \leq 1/10$.

The response to thermal load of case 2, obtained using plane strain solution, is presented in Table 2. It is observed that the ply-angle θ has a significant effect on all the displacement and stress components. The transverse shear stress $\hat{\tau}_{zx}$ is maximum at or near the interface of the piezoelectric layer with the substrate. The electric potential induced in the elastic substrate is found to be negligible for the thermal load case also. The FSDT and CLT solutions are compared with the plane strain solution for load case 2 in Fig. 3. It is observed that w and σ_x predicted by the 2D theories are in good agreement with the plane strain solution for very thin plates with $h/a=1/100$, but the error increases by large amount with increase in the thickness parameter h/a of the plate. The FSDT solution is not a significant improvement over the CLT solution for the thermal load case.

The response of the hybrid plates to electric potential load of case 3, using plane strain solution, is presented in Table 3. It is observed that for the potential load case also, the ply-angle θ has a significant effect on the displacement and stress components. However, the thickness parameter has the least effect on the displacements and the stresses as compared to the mechanical and thermal load cases. The transverse shear stress $\tilde{\tau}_{zx}$ is maximum at the

interface of the piezoelectric layer with the substrate. The CLT and the FSDT are assessed for load case 3 in Fig. 4. It is observed that the FSDT does not provide improved results compared to the CLT. Both the 2D solutions are in good agreement with the 3D solution, the error being less than 5% even for plates with $h/a \leq 1/10$.

The distributions of ϕ and D_z across the thickness of the piezoelectric layer, obtained by plane strain solution, are displayed in Fig. 5 for load cases 1 and 3. It is observed that the variation of ϕ is almost quadratic and that of D_z almost constant for the pressure load case. Their variations for the thermal load case 2, not displayed for brevity, are similar. For the potential load case 3, the variation of ϕ is almost linear and that of D_z almost constant. These variations can be adopted in 2D theories.

5. Conclusions

Analytical generalised plane strain solution is presented for cylindrical bending of simply supported angle-ply laminated plate subjected to thermoelectromechanical load. Numerical results are presented for hybrid plates made of a substrate of graphite-epoxy angle-ply laminated composite with a PZT-5A layer bonded to its top surface and subjected to sinusoidal loads. The displacements and the predominant stresses in the substrate are significantly affected by the ply-angle and the span-to-thickness ratio. The interface between the substrate and the piezoelectric layer is subjected to relatively higher shear stress for the thermal and the electrical potential loads. This may cause debonding of the piezoelectric layer. The CLT and the FSDT solutions are assessed. The FSDT solution is found to be an improvement over the CLT solution for plates under pressure load, the error being less than 5% for $h/a \leq 1/10$. The FSDT and the CLT solutions are good for plates under electrical load, the error being less than 5% for plates with $h/a \leq 1/10$. The FSDT solution for plates under thermal load is not an improvement over the CLT solution. Both these solutions are in close agreement with the plane strain solution for plates with $h/a=1/100$ under thermal load, but have large errors for plates with $h/a=1/40$. The variation of ϕ across the actuated piezoelectric layer is almost linear and across the unactuated one is almost quadratic.

References

Ashida, F., Noda, N. and Tauchert, T.R. (1994a), "A two-dimensional piezothermoelastic problem in an orthotropic plate exhibiting crystal class mm2", *JSME Int. Jnl. Series A*, **37**, 334-340.

Ashida, F., Noda, N. and Tauchert, T.R. (1994b), "Inverse problem of two-dimensional piezothermoelasticity in an orthotropic plate exhibiting crystal class mm2", *JSME Int. Jnl. Series A*, **37**, 341-346.

Brooks, B. and Heyliger, P. (1994), "Static behavior of piezoelastic laminates with distributed and patched actuators", *J. Intelligent Mat. Systems and Structures*, **5**, 635-646.

Dube, G.P., Kapuria, S. and Dumir, P.C. (1996), "Exact piezothermoelastic solution of simply-supported orthotropic flat panel in cylindrical bending", *Int. J. Mech. Sci.*, **38**, 1161-1177.

Heyliger, P. (1994), "Static behavior of laminated elastic/piezoelastic plates", *AIAA Jnl.*, **32**, 2481-2484.

Jonnalagadda, K.D., Blandford, G.E. and Tauchert, T.R. (1994), "Piezothermoelastic composite plate analysis using first-order shear-deformation theory", *Comput. Struct.*, **51**, 79-89.

Kapuria, S., Dube, G.P. and Dumir, P.C. (1997), "Exact piezothermoelastic solution for simply supported laminated flat panel in cylindrical bending", *ZAMM*, **77**, 281-293.

Pagano, N.J. (1970), "Influence of shear coupling in cylindrical bending of anisotropic laminates", *J. Composite Materials*, **4**, 330-343.

Ray, M.C., Rao, K.M. and Samanta, B. (1992), "Exact analysis of coupled electroelastic behavior of a piezoelectric plate under cylindrical bending", *Comput. Struct.*, **45**, 667-677.

Ray, M.C., Rao, K.M. and Samanta, B. (1993a), "Exact solution for static analysis of an intelligent structure under cylindrical bending", *Comput. Struct.*, **47**, 1031-1042.

Ray, M.C., Rao, K.M. and Samanta, B. (1993b), "Exact solutions for static analysis of intelligent structures", *AIAA Jnl.*, **31**, 1684-1691.

Tang, Y.Y., Noor, A.K. and Xu, K. (1996), "Assessment of computational models for thermoelectroelastic multilayered plates", *Comput. Struct.*, **61**, 915-933.

Tauchert, T.R. (1992), "Piezothermoelastic behavior of a laminated plate". *J. Thermal Stresses*, **15**, 25-37.

Xu, K., Noor, A.K. and Tang Y.Y. (1995), "Three-dimensional solutions for coupled thermoelectroelastic response of multilayered plates", *Comput. Methods Appl. Mech. Engrg.* **126**, 355-371.